Rock and Soil Mechanics

Volume 42 | Issue 12 Article 4

2-28-2022

Reliability of spatially variable earth slopes based on the upper bound analysis

Zhi-hao SUN
School of Resources and Environmental Engineering, Hefei University of Technology, Hefei, Anhui 230009, China

Xiao-hui TAN
School of Resources and Environmental Engineering, Hefei University of Technology, Hefei, Anhui 230009, China, tanxh@hfut.edu.cn

Zhi-bin SUN
School of Automotive and Transportation Engineering, Hefei University of Technology, Hefei, Anhui 230009, China

Xin LIN
School of Resources and Environmental Engineering, Hefei University of Technology, Hefei, Anhui 230009, China

See next page for additional authors

Custom Citation

SUN Zhi-hao, TAN Xiao-hui, SUN Zhi-bin, LIN Xin, YAO Yu-chuan, . Reliability of spatially variable earth slopes based on the upper bound analysis[J]. Rock and Soil Mechanics, 2021, 42(12): 3397-3406.

Reliability of spatially variable earth slopes based on the upper bound analysis

Authors

Zhi-hao SUN, Xiao-hui TAN, Zhi-bin SUN, Xin LIN, and Yu-chuan YAO

Rock and Soil Mechanics 2021 42(12): 3397−3406 ISSN 1000−7598
https: //doi.org/10.16285/j.rsm.2021.5569 rocksoilmech.researchcommons.org/journal

Reliability of spatially variable earth slopes based on the upper bound analysis

SUN Zhi-hao[1], TAN Xiao-hui[1], SUN Zhi-bin[2], LIN Xin[1], YAO Yu-chuan[1]
1. School of Resources and Environmental Engineering, Hefei University of Technology, Hefei, Anhui 230009, China
2. School of Automotive and Transportation Engineering, Hefei University of Technology, Hefei, Anhui 230009, China

Abstract: The spatial variability is an inherent uncertainty of soils. The random field theory is used to represent the spatial variability of soils, and the random field discretization is performed by the Karhunen-Loève (KL) expansion method. Using the slope upper bound analysis based on the discrete mechanism, the discretization results of the internal friction angle random field at each point in the space are considered when generating the velocity discontinuity surface. And the strength reduction technique, bisection searching, and sequential quadratic programming method are combined to solve the safety factor of slopes. The first-order reliability method (FORM) and subset simulation (SS) are employed for slope reliability analysis. Given the characteristics of SS and the shear strength reduction technique, an optimization algorithm coupling the two is proposed to improve computational efficiency. By calculating and analyzing an earth slope, the similarities and differences between FORM and SS based on the KL expansion method in solving the slope reliability index and failure consequence are clarified. The influence of the coefficient of variation of soil strength parameters on the slope reliability index and failure consequence is investigated, providing a theoretical basis for risk analysis and prevention of slopes.

Keywords: earth slope; upper bound analysis; spatial variability; first-order reliability method (FORM); subset simulation (SS)

1 Introduction

From the basic principle of plasticity mechanics, slope stability analysis can be divided into the upper and lower bound limit analysis. The upper bound limit analysis can strictly construct the kinematically admissible failure velocity field and has a rigorous theoretical foundation. At present, upper bound limit analysis is widely used in the stability analysis of slopes[1−7]. For non-homogeneous slopes, Wang et al.[5] investigated the application of upper limit analysis in the stability of non-homogeneous slopes with layered soil profiles. Luan et al.[6] explored the application of upper bound limit analysis in the stability analysis of non-homogeneous soil slopes under anti-sliding pile reinforcement conditions, assuming that the cohesion varies linearly with depth. Sun et al.[7] proposed a failure mechanism for the upper bound limit analysis of slopes based on the idea of spatial discretization, which can further consider the linear variation of the internal friction angle with depth. However, in most cases, the soil cohesion and internal friction angle are not simply linear with depth but are random fields with spatially variable properties.

The spatially variable properties of soil parameters such as cohesion and internal friction angle are also known as spatial variability or spatial autocorrelation, i.e., the properties of any two points in the soil layer are different but have some correlation, which is caused by different material composition, depositional environment, stress history, and climatic conditions. The spatial variability of soils can be described by the random field theory[8]. In order to obtain the specific realized value of the random field, random field discretization is required. The commonly used methods for random field discretization are the point discretization method, the local averaging subdivision, and the series expansion method[9−10]. Among them, the series expansion method expresses random fields as the sum of finite deterministic continuous functions without pre-partitioning the random field elements. As long as the coordinates of a point in space are given, the random field of geotechnical parameters at that point can be obtained by discretizing the random field.

The Karhunen-Loève expansion method (KL expansion method for short) is one of the series expansion methods, which is based on the spectral decomposition of the auto-covariance function for the discretization of random fields and has high computational efficiency and accuracy[10], so it is widely used in the reliability analysis of slope engineering. For example, Li et al.[11] used KL expansion method and finite element slip surface stress method for the reliability analysis of non-homogeneous slopes; Huang et al.[12] used a combination of KL expansion method and finite element limit analysis method for landslide risk analysis; Cho[13] used the KL expansion method and limit equilibrium method to study the influence of soil spatial variability on the slope stability. Li et al.[11] and Huang et al.[12] also pointed out that the volume of sliding mass can be estimated based on the slope critical slip surface location, which represents the failure consequence of slope instability for slope risk analysis. Most of these slope reliability and risk analysis use the limit equilibrium

Received: 15 April 2021 Revised: 21 August 2021
This work was supported by the National Natural Science Foundation of China (41972278; 42030710) and the National Key R & D Program of China (2019YFC1509903).
First author: SUN Zhi-hao, male, born in 1995, Master degree candidate, research interests: geotechnical reliability analysis. E-mail: szhh95@mail.hfut.edu.cn
Corresponding author: TAN Xiao-hui, female, born in 1971, PhD, Professor, doctoral supervisor, research interests: the geotechnical numerical simulation and reliability analysis. E-mail: tanxh@hfut.edu.cn

slice method or numerical analysis as deterministic analysis methods. Among them, the limit equilibrium slice method requires a pre-defined slip surface and a simplified assumption on the slice interaction force. The numerical analysis results may vary with the mesh refinement, and additional treatment is usually required to obtain the critical slip surface. Both methods have certain limitations for the stability analysis and critical slip surface determination of slopes with spatially variable soil.

As mentioned above, limit analysis, as an essential method for geotechnical structural analysis with rigorous plasticity mechanic assumptions, is widely used to solve slope stability. The technique requires the soil to strictly satisfy the associated flow law and cannot be directly applied to reliability problems considering the spatial variability of strength parameters. To avoid this difficulty, some scholars have studied the reliability of slopes with spatially variable soils using finite element limit analysis[14]. This theory can obtain the slope upper and lower bound limits of ultimate loads, but it requires similar element division and search optimization as finite element analysis when applied, which significantly increases the workload during reliability analysis. Therefore, this paper adopts the discrete upper bound limit mechanism proposed in recent years for reliability analysis of spatially variable slopes, which overcomes the applicability problems of traditional limit analysis in the study of such slopes and provides a new idea for the combination of limit analysis method and reliability analysis.

In summary, this paper proposes to combine the KL expansion method, upper bound limit analysis of non-homogeneous slopes based on the discrete mechanism and two commonly used reliability analysis methods (first-order reliability method (FORM) and subset simulation (SS)) for reliability analysis of spatially variable non-homogeneous slopes. Among them, the KL expansion method is used to carry out the discretization of random fields to obtain the soil strength parameters at arbitrary locations in space; the velocity discontinuity surface (sliding surface) is generated using the discrete mechanism, based on which the upper bound limit analysis, strength reduction method, sequential quadratic programming (SQP) algorithm and bisection method can be used jointly to analyze the slope by the fixed value method and calculate the slope safety factor; FORM and SS are used to solve the slope reliability index and failure consequence. Combining the characteristics of the strength reduction method and SS, this paper also proposes an optimization algorithm coupling them to improve the computational efficiency. Finally, the correctness of the method is verified by example analysis, and the influence of the variation coefficient of soil strength parameters on the slope reliability index and failure consequence is obtained.

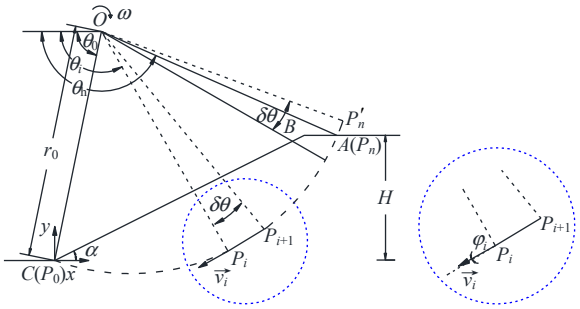

Fig. 1 Discrete mechanism for slope upper bound analysis

2 Upper bound limit analysis for slope stability

2.1 Discrete mechanism for slope upper bound limit analysis

As shown in Fig.1, the height of the slope is H, and the slope angle is α, AC is the velocity discontinuity surface of the upper bound limit analysis mechanism (i.e., the potential slip surface of the slope). Let the blocks above and below the velocity discontinuity surface be rigid bodies, and the sliding block ABC rotates around the point O with an angular velocity ω. Establish a rectangular coordinate system with C as the origin at the toe of the slope. θ_0 and θ_n are the angles between the points C and A on the velocity discontinuity surface and the negative x−axis, respectively, and r_0 is the radius from the point C to the center of rotation.

The slope upper bound limit analysis mechanism is based on the idea of spatial discretization[7]. In this mechanism, the velocity discontinuity surface consists of a series of straight-line segments (P_iP_{i+1}). Starting from the toe C (denoted as point P_0), a point-to-point approach is used to generate the velocity discontinuity surface from the toe to the crest of the slope until the ordinate y_{i+1} of P_{i+1} is greater than or equal to the slope height H. When $y_{i+1}>H$, the coordinates of P_{i+1} can be adjusted by the linear interpolation method so that P_{i+1} falls on the crest. According to the associated flow rule, the angle between the tangential velocity of the velocity discontinuity surface and the real velocity is required to be the soil friction angle, i.e., the angle between the vector $\overrightarrow{P_iP_{i+1}}$ and the velocity $\vec{v}_i$ of P_i is $(\pi-\varphi_i)$. Therefore, as shown in Fig.1, when the coordinate (x_i, y_i) of P_i is known, the coordinate (x_{i+1}, y_{i+1}) of P_{i+1} can be solved by the following equations:

$$x_{i+1}=x_i+\frac{\sqrt{(x_i-x_O)^2+(y_i-y_O)^2}\sin(\delta\theta)}{\sin(\pi/2+\varphi_i-\delta\theta)}\cdot\cos\left(\theta_i-\frac{\pi}{2}+\varphi_i\right) \tag{1}$$

$$y_{i+1}=y_i+\frac{\sqrt{(x_i-x_O)^2+(y_i-y_O)^2}\sin(\delta\theta)}{\sin(\pi/2+\varphi_i-\delta\theta)}\cdot\sin\left(\theta_i-\frac{\pi}{2}+\varphi_i\right) \tag{2}$$

where x_O and y_O are the coordinates of the rotation center point O; φ_i is the angle between P_i and the negative x−axis; φ_i is the soil internal friction angle at P_i; and $\delta\theta$ is the angle between two adjacent rays OP_i and OP_{i+1} (i.e., the angle between the two endpoints of the segment P_iP_{i+1} and the rotation center), which determines the accuracy of the generated velocity discontinuity surface. The results indicate that the method has sufficient computational accuracy when $\delta\theta = 0.1^{o}$[7].

As the origin of the coordinate is determined, the coordinate (x_O, y_O) of the rotation center O can be expressed by θ_0 and r_0. Therefore, for the discrete mechanism of slope upper bound limit analysis, when the angle $\delta\theta$ between two adjacent rays is assumed to be constant, the key parameters that determine the position of the velocity discontinuity surface are θ_0, r_0 and the soil internal friction angle φ.

2.2 Slope stability analysis

When using the upper bound limit theorem for slope stability analysis, it is necessary to calculate the external force power W and the internal energy dissipation D of the failure mechanism. As shown in Fig.2, the failure mechanism ABC is divided into n geometric discrete units P_iBP_{i+1} (i = 0, 1, …, n−1), then the external force power is the gravitational power of the soil mass W, which can be solved by the sum of the gravitational power W_i of each discrete unit. The internal energy dissipation D is the energy dissipation on the velocity discontinuity surface of the soil mass, which can be solved by the sum of the energy dissipation D_i of each discrete linear slip surface P_iP_{i+1}. The calculation formulas of W and D are as follows:

$$W = -\gamma\omega\sum S_i R_{Gi}\cos\theta_{Gi} \tag{3}$$

$$D = \omega\sum c_i L_i R_i \cos\varphi_i \tag{4}$$

where γ is the soil unit weight; ω is the angular velocity; S_i is the area of the discretized block P_iBP_{i+1}; R_{Gi} is the distance from the center of rotation O to the center of gravity of the discretized block P_{Gi}; θ_{Gi} is the angle between OP_{Gi} and the negative x−axis; R_i is the distance from the center of rotation O to the point P_i; L_i is the length of the linear slip surface P_iP_{i+1}; and c_i and φ_i are the cohesion and the internal friction angle at the starting point P_i of the i−th linear slip surface, respectively.

In the upper bound limit analysis, the slope safety factor can be obtained by the strength reduction method. Let the strength reduction factor be F_s, and the reduced cohesion and internal friction angle be c_R and φ_R, respectively, then:

$$c_R = c/F_s,\quad \varphi_R = \tan^{-1}(\tan\varphi/F_s) \tag{5}$$

In calculating the slope energy dissipation, it is necessary to substitute the reduced strength parameters into Eq.(4) for analysis. At this time, the key parameters that determine the location of velocity discontinuity surface are θ_0, r_0 and φ_R. Hence, the location of velocity discontinuity surface and the slope energy dissipation function $f_{WD} = |W-D|$ are functions of parameters θ_0, r_0, F_s, c and φ.

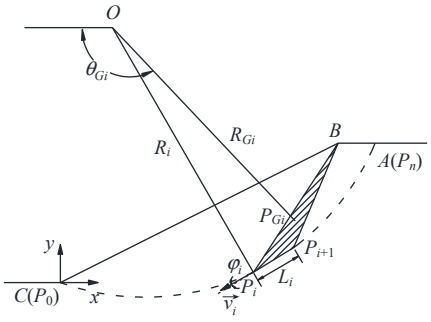

Fig. 2 Power calculation of the discrete unit

According to the upper bound theorem, if a set of parameters θ_0, r_0, and F_s exist and make slope energy dissipation function f_{WD}=0, the slope is in the limit state; otherwise, the slope is in the stable condition. When c, φ and F_s are known, f_{WD} is a function of θ_0 and r_0, so the solution of the slope safety factor F_s is a multivariate optimization problem. In this paper, the nonlinear sequence quadratic programming (SQP) method is used for the optimal solution of f_{WD}, and the critical strength reduction factor is searched for by the bisection method as the slope safety factor F_s. The specific steps of the strength reduction method are described in the literature [7], and the convergence criterion of the safety factor is taken as 0.001 in this paper.

3 Slope reliability analysis considering spatial variability of soil properties

3.1 Random field model describing spatial variability

Assume that the cohesion and the internal friction angle obey two-dimensional stationary log-normal random fields, and then the number of random fields N = 2. The spatial variability of soils is often represented by an autocorrelation function of the following form[15]:

$$\rho(\boldsymbol{x}_1, \boldsymbol{x}_2) = \exp\left[-\left(\frac{\Delta x}{L_h}\right)^2 - \left(\frac{\Delta y}{L_v}\right)^2\right] \tag{6}$$

where $\boldsymbol{x}$=[x, y] is the spatial coordinate; Δx and Δy are the horizontal and vertical distances between any two points in the space, respectively; and L_h and L_v are the autocorrelation distances in the horizontal and vertical coordinate directions, respectively.

According to the basic principle of the KL expansion method, the discrete results of a log-normal random field can be expressed as:

$$\hat{H}_i(\boldsymbol{x}) = \exp\left(\mu_{\ln X_i} + \sigma_{\ln X_i}\sum_{j=1}^{M}\sqrt{\lambda_j}f_j(\boldsymbol{x})(\xi L^{\mathrm{T}})_{ji}\right) \tag{7}$$

where $\hat{H}_i(\boldsymbol{x})$ is the random field discretized value at a point x in the space; M is the number of terms of the KL expansion method; λ_j and $f_j(\boldsymbol{x})$ are the j-th eigenvalue and eigenfunction (j = 1, 2, …, M) of the autocorrelation function $\rho(\boldsymbol{x}_1, \boldsymbol{x}_2)$, respectively; $\boldsymbol{\xi}$ is a matrix of size $M \times N$ whose elements are independent standard normal random variables; $\boldsymbol{L}$ is the lower triangular matrix obtained from the Cholesky decomposition of the mutual correlation matrix $\boldsymbol{R}_{\mathrm{Y}}$ with a size of $N \times N$ in the associated standard normal space ($\boldsymbol{Y}$ space); the superscript T denotes the transpose of the matrix; the relational expression of $\boldsymbol{R}_{\mathrm{Y}}$ and $\boldsymbol{R}_{\mathrm{X}}$($\boldsymbol{R}_{\mathrm{X}}$ is the mutual correlation matrix in the original space $\boldsymbol{X}$) is given in the reference [16]; and $\mu_{\ln X_i}$ and $\sigma_{\ln X_i}$ are the mean value and the mean square deviation after normalization for the i−th (i = 1, 2, …, N) random field, which can be calculated as follows:

$$\left.\begin{aligned}\sigma_{\ln X_i} &= \sqrt{\ln(1+\delta_{X_i}^2)} = \sqrt{\ln(1+(\sigma_{X_i}/\mu_{X_i})^2)} \\ \mu_{\ln X_i} &= \ln\left(\mu_{X_i}\Big/\sqrt{1+\delta_{X_i}^2}\right) = \ln\mu_{X_i} - \frac{1}{2}\sigma_{\ln X_i}^2\end{aligned}\right\} \tag{8}$$

where $\mu_{\ln X_i}$ and $\sigma_{\ln X_i}$ are the mean value and the mean square deviation for the i−th random field, respectively.

It can be seen from Eqs. (7) and (8) that the key of the KL expansion method is to determine the eigenvalue, the eigenfunction, and the number of expansion terms M for the autocorrelation function. Among them, the eigenvalue and the eigenfunction are jointly determined by the autocorrelation function and the definition domain of the random field.

The number of expansion term M can be determined from the random field discretization error ε_{d} and its allowable error $\varepsilon_{\mathrm{d0}}$, where the discrete error is calculated as[17]:

$$\varepsilon_{\mathrm{d}} = 1 - \frac{1}{S}\sum_{j=1}^{M}\lambda_j \tag{9}$$

where S is the area of the discrete region of the random field. From Eq.(9), it can be seen that the discretization error ε_{d} decreases with the increase of the number of expansion term M. In order to balance the computational accuracy and efficiency, the minimum M value satisfying $\varepsilon_{\mathrm{d}} \leqslant \varepsilon_{\mathrm{d0}}$ can be taken as the optimal number of expansion term.

3.2 Reliability analysis method based on the KL expansion method

Without loss of generality, the slope performance function is taken as:

$$Z = g(\boldsymbol{X}) = F_{\mathrm{s}}(\boldsymbol{X}) - 1 \tag{10}$$

where $\boldsymbol{X} = [X_1, \ldots, X_n]$($i$ = 1, 2, …, n) is the basic variable; and n is the number of basic variable.

From Eq.(7), it can be seen that after the random field is discretized by the KL expansion method, the continuous random field can be represented by a random vector matrix ξ of size $M \times N$. Considering the elements of ξ as the basic variables X in the reliability analysis, the KL expansion method can be combined with various conventional reliability analysis methods to perform the reliability analysis of slopes.

In the discrete mechanism of the slope upper bound limit analysis, the velocity discontinuity surface AC consists of a series of linear segments (P_iP_{i+1}), and the position of AC is determined by the variables representing the center of rotation (θ_0 and r_0), while the direction of each segment P_iP_{i+1} in AC is determined by the internal friction angle φ_i at the point P_i. Therefore, when considering the spatial variability of soil, it is convenient to combine the discretization of random field with the generation of velocity discontinuity, then the slope safety factor can be solved based on the discretization mechanism of upper bound analysis, and the reliability analysis of slope can be conducted on this basis.

The main steps of slope reliability analysis by combining upper bound limit analysis and the KL expansion method are as follows.

(1) Solve the eigenvalues and eigenfunctions in Eq.(7) using the KL expansion method for the slope geometry and the soil spatially variable property.

(2) Determine the number of KL expansion term M of the random field according to $\varepsilon_{\mathrm{d}} \leqslant \varepsilon_{\mathrm{d0}}$ and the discretization error expression (Eq.(9)).

(3) Generate a single realization for the random vector matrix ξ.

(4) Substitute the eigenvalues, eigenfunctions, and realizations of the random vector matrix determined in steps (1) and (3) into Eq.(7) to obtain a realization of the discrete value function $\hat{H}_i(\boldsymbol{x})$ of the random field.

(5) The slope safety factor is calculated jointly using the strength reduction method, the bisection method and the SQP method.

It should be noted that the process of generating the random vector matrix in step (3) is related to the reliability analysis method. When the KL expansion method is combined with FORM, the random vector matrix values can be obtained from the iterative calculation of FORM, and the detailed iterative calculation process is described in the reference [15]; when the KL expansion method is combined with SS, the random vector matrix values are generated randomly by the operation rules of SS. The related theory of SS and the optimization algorithm of SS coupled with the strength reduction method are described below.

3.2.1 Brief introduction of SS

SS[18] is an advanced Monte Carlo simulation (MCS) method that can efficiently estimate the probability of failure for high-dimensional small-probability events. Its central idea is that the probability $P(F)$ of occurrence for a small-probability event F is expressed as the product of large conditional probabilities of a series of intermediate

failure events according to the conditional probabilities, that is

$$P_{\mathrm{f}} = P(F) = P(F_1) \cdot \prod_{i=2}^{m} P(F_i \mid F_{i-1}) \tag{11}$$

where the intermediate failure event is $F_i = \{Z \leqslant b_i\}$ (i = 1, 2, …, m); Z is the performance function value of the event; b_i is the critical performance function value of the intermediate failure event (referred to as threshold); $P(F_i)$ is the occurrence probability of the event F_i; and $P(F_i|F_{i-1})$ is the occurrence probability of F_i occurring under the condition that the event F_{i-1} occurs. Let $b_1 > b_2 > \ldots > b_{m-1} > b_m = 0$, then the intermediate failure events have the inclusion relation, $F_1 \supset F_2 \supset \ldots \supset F_{m-1} \supset F_m$.

In the process of SS, the threshold b_i for intermediate failure events can be determined automatically based on the value of the performance function corresponding to the conditional probability sample such that both $P(F_1)$ and $P(F_i|F_{i-1})$ (i = 2, 3, ..., m-1) are equal to the specified conditional probability p_0, where the intermediate failure conditional samples of events are generated by Markov Chain Monte Carlo simulation (MCMC for short)[19].

The main steps of SS are as follows:

(a) The first layer of SS (random sampling layer): generate N_{s} samples randomly, calculate the performance function value corresponding to each sample, and determine the N_s function value of the p_0×100-th percentile as the threshold b_1 of the intermediate failure event F_1. The process of determining the p_0×100-th percentile is as follows: first sort the N_s performance function values in ascending order; then determine the p_0N_{s}-th and the p_0N_{s}+1-th performance function values according to the sorting results and total sample number N_{s}; finally, the mean value of these two performance function values is taken as the p_0×100-th percentile. The sample corresponding to the first p_0N_{s} minimum performance function value after sorting is selected as the seed sample of F_1. Among the N_s samples in the first layer, there are a total of p_0N_{s} performance function values of sample points less than or equal to the threshold b_1, so the conditional probability $P(F_1) = p_0$ is satisfied.

(b) The i−th layer of SS ($i \geqslant 2$, conditional sampling layer): N_{s}−p_0N_{s} conditional samples are generated using MCMC for the p_0N_{s} seed samples obtained at the i−1-th layer. The function values of all N_{s} samples (including p_0N_{s} seed samples and newly generated $N_{\mathrm{s}}(1-p_0)$ samples) are used to calculate the threshold b_i of the intermediate failure event F_i by the method of determining the p_0×100-th percentile in step (a); the samples corresponding to the first p_0N_{s} minimum performance function values after sorting are selected as the seed samples for the next layer of SS. Among the N_{s} samples at the i−th layer, a total of p_0N_{s} sample points have performance function values less than or equal to the threshold b_i, and therefore also satisfy the conditional probability $P(F_i|F_{i-1}) = p_0$.

(3) Repeat step (b) until the p_0×100-th percentile function value of the layer satisfies $b_i \leqslant 0$. Let the layer be the m-th layer of SS and let $b_m = 0$. Count the number of sample points N_{f} in this layer whose function value is less than or equal to 0, then $P(F_m|F_{m-1}) = N_{\mathrm{f}}/N_{\mathrm{s}}$.

According to the above steps, Eq.(11) can be simplified as:

$$P_{\mathrm{f}} = p_0^{m-1}(N_{\mathrm{f}}/N_{\mathrm{s}}) \tag{12}$$

where m is the number of SS layers; and N_{s} is the number of samples required for each layer of SS. In SS, the conditional probability p_0 = 10% is commonly taken[19], then for a failure event with a magnitude of 10^{-m}, a total of m layers of SS need to be executed, the corresponding calculation times of the performance function is:

$$N_{\mathrm{T}} = N_{\mathrm{s}} + (m-1)(1-p_0)N_{\mathrm{s}} = N_{\mathrm{s}}(0.9m + 0.1) \tag{13}$$

After the failure probability of slope is obtained, the slope reliability index can be calculated by the following formula:

$$\beta = -\Phi^{-1}(P_{\mathrm{f}}) \tag{14}$$

3.2.2 Optimization algorithm coupling SS and strength reduction method

Compared with the direct MCS, SS has higher computational efficiency. However, the essence of SS is a simulation-based reliability analysis method. In order to obtain more accurate simulation results, at least several thousand simulations are generally required, and each simulation needs to call the fixed value method procedure to solve the slope safety factor. According to the derivation in Section 2, the slope safety factor of the discrete mechanism based on the upper bound limit analysis needs to be solved by a combination of strength reduction method, bisection method, and optimization method. For each strength reduction factor in the bisection method, the SQP method needs to be called in the upper bound limit analysis to solve the minimum value of the energy dissipation function $f_{\mathrm{WDmin}} = \min|W-D|$, which is relatively large and requires several iterations. To address the problem of the low computational efficiency of the strength reduction method in SS, Huang et al.[20] used the value of yield function to measure the safety of slopes, which avoids a large number of iterations in solving the slope safety factor by bisection method and improves the computational efficiency. However, this method is only applicable to the slope stability analysis based on the elastoplastic finite element method. The calculation process of the upper bound limit analysis of slope stability adopted in this paper does not involve yield function, so the improved method cannot be applied. For this reason, this paper proposes an optimization algorithm coupled with SS and strength reduction method starting from reducing the bisection number of the strength reduction factors in order to reduce the computational cost of slope reliability analysis and improve the computational efficiency. The proposed optimization method is mainly based on the following

two reasons.

On the one hand, SS uses MCMC to generate conditional samples $\boldsymbol{\xi}_1$ based on the current sample $\boldsymbol{\xi}_0$. The brief process is to generate the underlying samples v based on the current sample $\boldsymbol{\xi}_0$ and calculate the corresponding performance function value, and if the performance function value is within the threshold of the target intermediate failure event, let $\boldsymbol{\xi}_1 = v$, otherwise let $\boldsymbol{\xi}_1 = \boldsymbol{\xi}_0$. For the conditional sampling layer of SS, the underlying sample v generated by MCMC has approximately a probability of 56% will be determined to be outside the target threshold and discarded[19], at which point there is no need to calculate the specific performance function values of these discarded samples. Therefore, in the bisection process of strength reduction method, if a conditional sample can be quickly judged to be outside the target threshold, the bisection process of strength reduction method can be ended in advance, and the computational efficiency can be improved.

On the other hand, from the calculation process of SS in Section 3.2.1, it is known that the threshold value b_i of an intermediate failure event is determined by the p_0N_s-th and the p_0N_s+1-th values after sorting the sample performance function values from smallest to largest, similar to the idea in the previous section if the performance function value of a sample can be quickly judged to be greater than the p_0N_s+1-th sample function value, then the true function value of the sample does not influence the threshold value b_i, and the process of solving the slope safety factor can be ended in advance. Therefore, after the number of sample points is greater than p_0N_s+1, a threshold $b_{i,j}$ can be set to be adjusted dynamically with the increase of sample points. The dynamic threshold $b_{i,j}$ can be expressed by the p_0N_s+1-th performance function value after the ascending order of the known sample performance function values, and $b_{i,j}$ has a tendency to decrease with the increase of sample points.

Combining the above two aspects, the following two points are optimized in this paper for the algorithm coupling SS and strength reduction method.

(1) Optimization 1

For each conditional sample generated by SS conditional sampling layer (i.e., the i−th layer of SS, $i \geqslant 2$), whether the true value of slope safety factor F_s meets $F_s - 1 > b_{i-1}$ is decided according to the threshold value b_{i-1} of the i−1-th intermediate failure event. If it is, it means that the sample point is not in the domain of the target event $F_{i-1} = \{Z \leqslant b_{i-1}\}$, and its safety factor is taken as any value greater than $1 + b_{i-1}$ and the solving process of the slope safety factor is exited; otherwise, it is necessary to update the upper limit of safety factor of bisection method to $1 + b_{i-1}$ and continue to calculate the slope safety factor. Of which, the method to determine whether F_s meets $F_s - 1 > b_{i-1}$ is as follows: let the strength reduction factor be $1 + b_{i-1}$, and reduce the strength parameters according to Eq. (5); use the SQP method to search the minimum slope energy dissipation f_{WDmin}. If $f_{WDmin} > 0$, it indicates that the true slope safety factor is $F_s > 1 + b_{i-1}$.

(2) Optimization 2

In the sample generation at the i-th layer of SS (i = 1, 2, …, m), with the increase of simulation numbers, when the number of performance functions obtained (the conditional sampling layer includes the known N_sp_0 seeds) meets $j \geqslant N_sp_0 + 1$, the dynamic threshold $b_{i,j}$ will also be updated correspondingly. When calculating the performance function value for the j+1-th sample, it should be judged that whether the true slope safety factor F_s meets $F_s > 1 + b_{i,j}$: if it is, the sample point does not belong to the intermediate event $F_i = \{Z \leqslant b_i\}$, the true safety factor has no impact on the result of SS, the value in the field $(1 + b_{i,j}, 1 + b_{i-1}]$ can be used as the safety factor; if it is not, it is necessary to update the upper limit of the safety factor of bisection method to $1 + b_{i,j}$, and continue to solve the safety factor. It is worth noting that when the updated dynamic threshold $b_{i,j} \leqslant 0$, it indicates that SS has entered into the m-th layer. At this time, let the dynamic threshold $b_{m,j}$ of the SS layer be always 0.

To sum up, the optimization algorithm proposed in this paper is based on the different influence of F_s in the SS process, and ending F_s true value search process of some samples in advance to improve the computational efficiency. Although Optimization 2 will lead to partial distortion of the cumulative distribution obtained by SS, it has no influence on the SS process, the failure probability, and the failure sample.

When combining the optimization algorithm with the upper limit analysis for reliability analysis of slope stability, the computational flow is shown in Fig.3. Fig.3(a) shows the flowchart of the main procedure of the subset simulation method, which is used to carry out the reliability analysis and solve for the failure probability of slopes, including the dispersion of random fields, the solution of safety factors and the determination of the threshold value of each subset layer. Among them, the most computationally intensive is the step of solving the slope safety factor (also known as solving the performance function) using the bisection method (see the thick box in Fig.3(a)), which can be realized by calling the subroutine (dotted box) in Fig.3(b). Fig.3(b) shows the flowchart of the subroutine for solving the slope safety factor by the fixed-value method, including judging whether the newly generated sample using MCMC is within the target threshold (long dashed box), estimating the threshold of intermediate failure events and judging whether the sample is within the estimated domain of intermediate failure events (short dashed box).

4 Examples

4.1 Slope reliability index and failure consequence

The earth slope under consideration has a height of

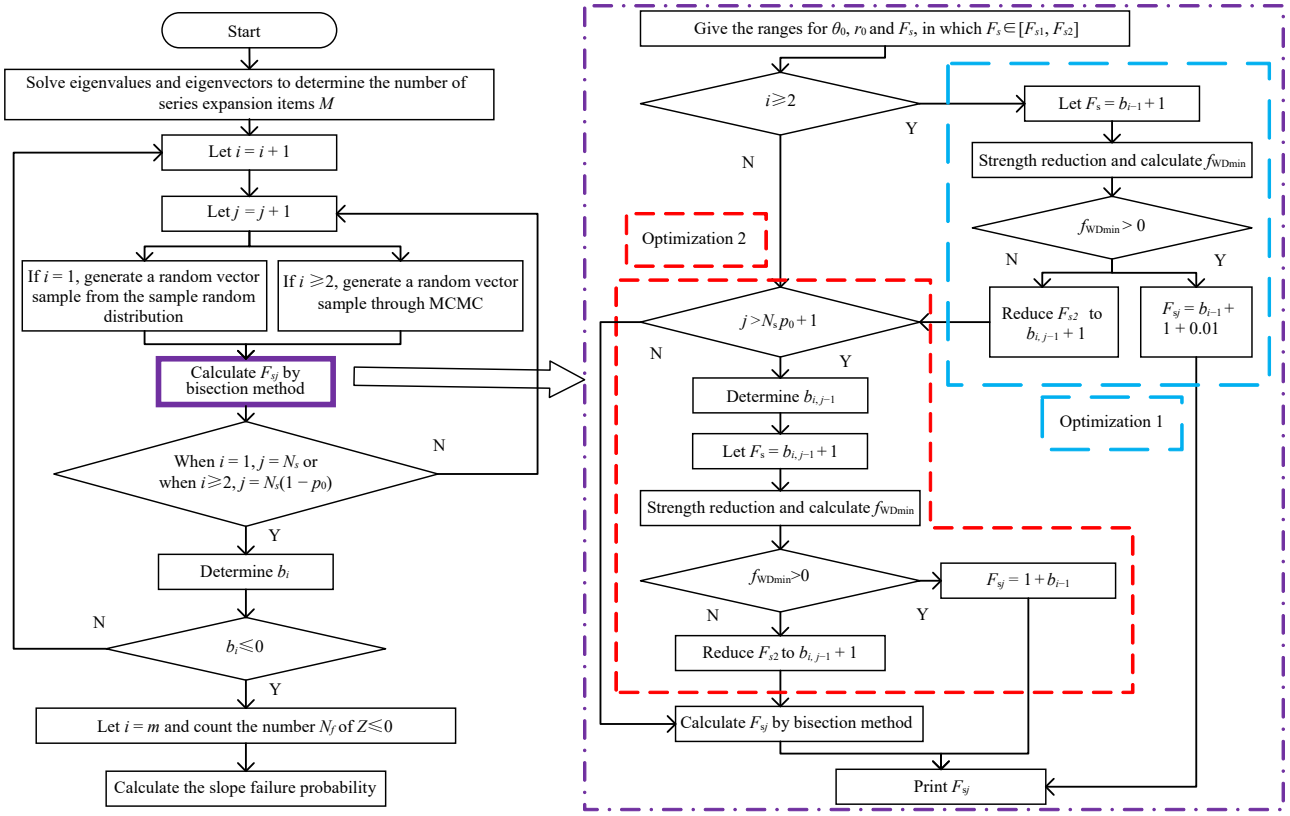

(a) Main program flowchart for failure probability calculation by SS (b) Subroutine flowchart for safety factor calculation

Fig. 3 Flowchart of Subset Simulation based on the optimization algorithm

10 m, the slope ratio is 1∶2, and the soil unit weight is 20 kN /m³. The cohesion and internal friction angle are random fields obeying log-normal distributions, their statistical probability parameters are shown in Table 2, and the autocorrelation function is of exponential square type. The reliability analysis of the slope is carried out by FORM and SS, respectively, where the sample number per level of SS N_s = 1 000.

Table 1 Probability distribution characteristic of soil parameters

Parameter	Mean value	Coefficient of variation δ	L_h /m	L_v /m
Cohesion c	10 kPa	0.3	30	3
Internal friction angle φ	20°	0.2	30	3

4.1.1 Reliability index

For the random field method, when $L_h = L_v = \infty$, the random field degenerates to random variable, therefore, the correctness of the method in this paper can be verified by comparing the reliability index of the random variable method with that of the random field method when $L_h = L_v = \infty$. Table 2 shows the reliability analysis results of the slope under three conditions, where M denotes the number of expansion term which is obtained from whether the discretization error of the random field satisfies $\varepsilon_d \leqslant \varepsilon_{d0} = 5\%$; N_Z denotes the number of solving the performance function in the reliability analysis process, that is, the number of calls to the subroutine for solving the slope safety factor in the upper bound limit analysis; MCS denotes the Monte Carlo simulation method, which is used to verify the calculation accuracy of FORM and SS.

As can be seen from Table 2, for the random variable method and the random field method at $L_h = L_v = \infty$, the reliability indexes obtained using FORM, SS and MCS are very close, which shows the correctness of the method in this paper. The slight differences are caused by the different specific solution process of FORM, SS, and MCS and the discretization error of the random field. Comparing the calculation results of FORM, SS, and MCS under the baseline conditions shown in Table 1, the difference between the reliability indexes of FORM and MCS is about 4.2%, and the difference between the reliability indexes of SS and MCS is about 3.8%, which shows that the reliability indexes of the three are consistent, proving that the KL-based FORM and SS in this paper have better calculation accuracy. From Table 2, it can also be seen that the reliability index of slope has a large increase when considering the spatial variability of soil, so the influence of soil spatial variability should be considered in slope stability analysis, otherwise, overly conservative results will be obtained.

As for the computational efficiency, it can be seen from Table 2 that the number of calls N_z of FORM for solving the safety factor subroutine is much smaller than that of SS under the three computational conditions,

indicating that the KL expansion-based FORM can be well applied to the slope reliability analysis considering soil spatial variability. For another, although the value of N_z of SS is greater than the corresponding value of FORM, for the optimized SS, the bisection searching process is ended earlier for many samples in the process of calculating the slope safety factor, which contributes to improving the computational efficiency of SS. Take the SS calculation process of the random field method (L_h = 30 m，L_v = 3 m) in Table 2 as an example: in the process of sample generation at the first level of SS, the dynamic threshold b_1 avoids the process of solving the true performance function values for 673 samples (only 1 strength reduction is required); in the process of sample generation at the second level of SS, by judging the sample function values outside the b_1 domain, the process of solving the real performance function values for 459 samples is avoided (only 1 strength reduction is required); the process of solving the real performance function values of 281 samples is avoided by the dynamic threshold b_2 (only 2 strength reductions are required). It can be seen that for the 1 900 samples generated in the SS process, 1 132 samples require only 1 strength reduction and 281 samples require only 2 strength reductions. Thus, the optimization algorithm speeds up the process of solving the failure probability and obtaining failure samples for SS.

Table 2 Slope reliability index and failure consequence

Reliability analysis method		M	N_Z	Reliability index β	Sliding volume /(m³ • m⁻¹)
Random variable method	FORM	—	15	1.65	70.27
	SS	—	1 900	1.68	70.56
	MCS	—	10 000	1.67	70.77
Random field method ($L_h = L_v = \infty$)	FORM	1	15	1.65	70.04
	SS	1	1 900	1.68	71.34
	MCS	1	10 000	1.67	70.55
Random field method (L_h = 30 m, L_v = 3 m)	FORM	18	438	2.28	71.92
	SS	18	1 900	2.29	75.26
	MCS	18	10 000	2.38	75.11

4.1.2 Failure consequence

In the slope reliability analysis, both the slope reliability index and the location of critical slip surface need to be determined. The slope failure probability can be solved based on the reliability index; the volume of slope failure can be estimated according to the location of the critical slip surface of the slope failure sample, which can be used to characterize the consequences of slope failure[11−12]. Estimating the slope failure probability and failure consequences is a prerequisite for slope risk analysis.

The reliability analysis of the slope using FORM can obtain the critical slip surface, which is corresponding to the critical failure mode of the slope when the iterative calculation of the reliability index reaches stability (see the dashed line in Fig.4). For the plane strain analysis, the area enclosed by the slip surface and the outside surface of the slope represents the volume of the sliding mass. The essence of SS is a simulation sampling, and it can only obtain the critical slip surface of the slope under different sampling conditions like MCS (see the multiple black solid lines in Fig.4), but SS can easily obtain more failure samples through MCMC to estimate the failure consequences of multiple failure modes of the slope more accurately[11]. In this case, the mean value of the sliding volume for all failure modes of SS can be taken as the slope failure consequence indicator[11]. The slope sliding volumes under the three calculation conditions are shown in Table 2. It can be seen that for the random variable method and the random field method with $L_h = L_v = \infty$, the sliding volumes calculated by FORM, SS and MCS are consistent and their values are slightly smaller than that of the random field method under the baseline condition. This indicates that the failure consequence of the slope increases slightly when the soil spatial variability is considered. Therefore, the influence of soil spatial variability should be considered in the slope stability analysis, otherwise the slope failure consequences will be underestimated to some extent.

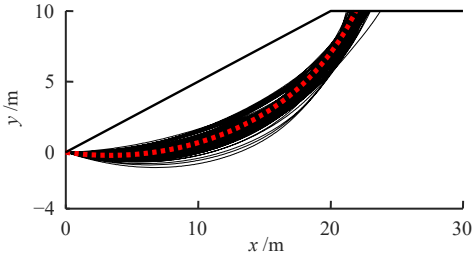

Fig. 4 Location of critical slip surfaces

4.2 Sensitivity analysis of slope reliability index and failure consequence

Based on the benchmark conditions shown in Table 1, the relationships between the slope reliability index, failure consequence, slip surface location and the coefficients of variation of strength parameters are studied when the coefficients of variation of the cohesion and internal friction angle vary between 0.1 and 0.4, respectively, and the results are shown in Figs 5−7.

As seen in Fig.5(a), the reliability indexes obtained by FORM and SS are basically the same for the same coefficient of variation, which again proves the correctness of the slope reliability analysis method based on the discrete upper bound limit mechanism in this paper. It can also be seen from this figure that the reliability index of the slope decreases with the increase of the coefficient of variation of the soil strength parameter. When the coefficient of variation of internal friction angle δ_φ = 0.2, the reliability index of the slope decreases slowly with the increase of δ_c. When the coefficient of variation of cohesion δ_c = 0.3, the reliability index of the slope decreases rapidly with the increase of δ_φ. Therefore, the slope reliability index is more sensitive to the coefficient of variation of internal friction angle.

As seen in Fig.5(b), for the same coefficient of variation, the slope failure consequences obtained by FORM and SS differ from each other, and the failure consequences of the former are smaller than those of the latter in most cases, which is caused by the inherent difference of calculating the critical slip surface and failure consequence in FORM and SS. However, under the same conditions, the slope failure consequences derived from FORM and SS are consistent with the change of coefficients of variation. For example, when the coefficient of variation of internal friction angle $\delta_\varphi = 0.2$, the slope failure consequence decreases with the increase of δ_c. When the coefficient of variation of cohesion $\delta_c = 0.3$, the slope failure consequence increases with the increase of δ_φ.

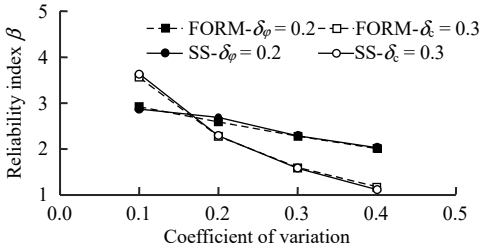

(a) Relationship between the coefficient of variation and the reliability index

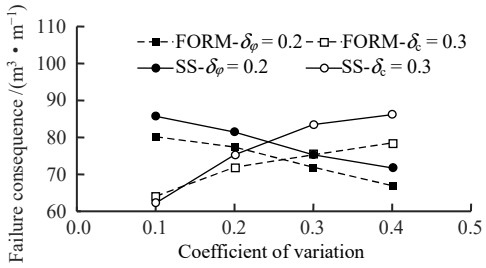

(b) Relationship between the coefficient of variation and the failure consequence

Fig. 5 Influence of coefficient of variation on the reliability index and failure consequence of slope

The variation shown in Fig.5(b) can be further explained by Figs. 6−7. In Figs. 6−7, the dashed line is the location of the critical slip surface of FORM, and the multiple black solid lines indicate the location of the critical slip surface obtained by SS. When $\delta_\varphi = 0.2$, with the increase of δ_c, the position of the dashed line in Fig.6 shifts slightly upward, i.e., the consequence of slope failure decreases slightly with the increase of δ_c; when $\delta_c = 0.3$, the position of the dashed line in Fig.7 moves downward with the increase of δ_φ, i.e., the consequence of slope failure slightly increases with the increase of δ_φ. It can also be seen from Fig.7 that the fluctuation range of the critical slip surface position increases with the increase of δ_φ. Considering this variation in the prevention and control of slopes is helpful and more reasonable for slope supporting designs.

The relationship between the slope failure consequence and the coefficient of variation of soil strength parameters shown in Figs. 5−7 is related to the log-normal distribution of strength parameters. Taking SS as an example, the

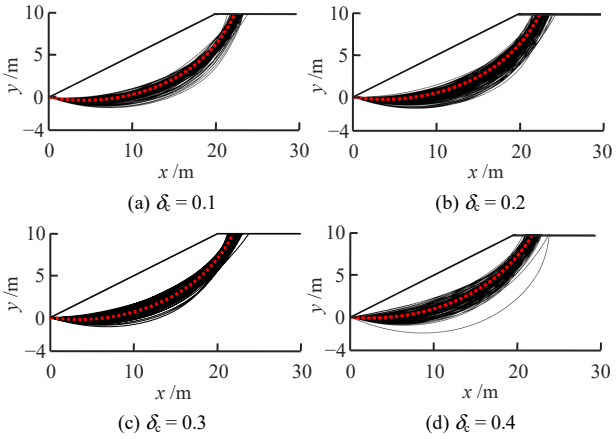

Fig. 6 Slope critical slip surface under different variation coefficients of cohesion ($\delta_\varphi = 0.2$)

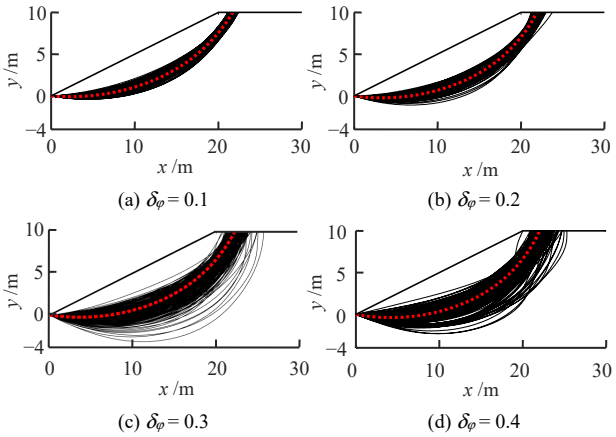

Fig. 7 Slope critical slip surface under different variation coefficients of internal friction angle ($\delta_c = 0.3$)

frequency distribution of the dispersion results of cohesion adjacent to the slip surface is plotted under different coefficients of variation, and the results are shown in Fig.8. This figure shows that the dispersion of cohesion increases with the increase of the coefficient of variation, and its mode shifts to the left, and the non-normality is more obvious. The internal friction angle also obeys the log-normal random field, and its frequency distribution varies with the coefficient of variation in a similar manner to Fig.8. The literature [21] states that for a given slope geometry, the slip surface location is only related to the dimensionless parameter $\lambda_{c,\varphi} = c/(\gamma h \tan\varphi)$, and the sliding surface depth increases with $\lambda_{c,\varphi}$. This indicates that a decrease in cohesion leads to a reduction in slip surface

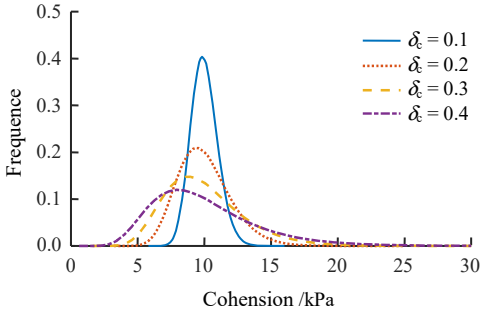

Fig. 8 Frequency distribution of the discretized cohesion

depth, while a decrease in internal friction angle leads to an increase in slip surface depth. Therefore, the slope failure consequence decreases with the increase in the coefficient of variation of the cohesion and increase with the increase in the coefficient of variation of the internal friction angle.

5 Conclusions

In order to consider the spatial variability of soils in the slope stability analysis, the paper improves the discrete mechanism of the upper limit analysis of the slope by combining it with the KL expansion method of random field dispersion, which can consider the influence of the spatial variability of the soil friction angle on the position of the slip surface when generating the velocity interrupted surface. On this basis, an optimization algorithm coupling subset simulation (SS) and strength reduction method is proposed, and the slope stability analysis is carried out using FORM and SS based on the optimization algorithm respectively, and the relationship between the slope reliability index and the failure consequence and the coefficient of variation of strength parameters are obtained. The main conclusions of the paper are as follows.

(1) The discrete mechanism of slope upper limit analysis can be conveniently incorporated with random field method for reliability analysis of slopes with spatially variable soil.

(2) SS based on the optimization algorithm can end the bisection calculation process of strength reduction coefficient in advance when the conditions are satisfied, and improve the computational efficiency of SS to a certain extent.

(3) The slope reliability indexes obtained by FORM and SS are close to each other, whereas the slope failure consequences obtained by FORM are generally smaller than the corresponding values of SS.

(4) The slope reliability index decreases with the increase of the coefficients of variation of internal friction angle and cohesion, among which the reliability index is more sensitive to the change of the coefficient of variation of internal friction angle.

(5) In the log-normal random fields, the slope failure consequence decreases with the increase of coefficient of variation of cohesion and increases as the coefficient of variation of internal friction angle increases.

References

[1] LIU Feng-tao, ZHANG Shao-fa, DAI Bei-bing, et al. Upper bound limit analysis of soil slopes based on rigid finite element method and second-order cone programing[J]. Rock and Soil Mechanics, 2019, 40(10): 4084−4091, 4100.

[2] HUANG Wen-gui, LEONG Eng-choon, RAHARDJO Harianto. Upper-bound limit analysis of unsaturated soil slopes under rainfall[J]. Journal of Geotechnical and Geoenvironmental Engineering, 2018, 144(9): 04018066- 1-04018066-10.

[3] GAO Yu-feng, SONG Wen-zhi, ZHANG Fei, et al. Limit analysis of slopes with cracks: comparisons of results[J]. Engineering Geology, 2015, 188: 97−100.

[4] TANG Gao-peng, ZHAO Lian-heng, LI Liang, et al. Stability charts of slopes under typical conditions developed by upper bound limit analysis[J]. Computers and Geotechnics, 2015, 65: 233−240.

[5] WANG Zhen, CAO Lan-zhu, WANG Dong. Evaluation on upper limit of heterogeneous slope stability[J]. Rock and Soil Mechanics, 2019, 40(2): 323−328.

[6] LUAN Mao-tian, NIAN Ting-kai, YANG Qing. Stability analysis of pile-stabilized slopes considering both nonhomogeneity and anisotropy of soil strength using upper bound method of limit analysis[J]. Rock and Soil Mechanics, 2006, 27(4): 530−536.

[7] SUN Zhi-bin, PAN Qiu-jing, YANG Xiao-li, et al. Discrete mechanism for upper bound analysis of nonhomogeneous slopes[J]. Chinese Journal of Rock Mechanics and Engineering, 2017, 36(7): 1680−1688.

[8] VANMARCKE E H. Probabilistic modeling of soil profiles[J]. Journal of the Geotechnical Engineering Division, 1977, 103(11): 1227−1246.

[9] PHOON K K, HUANG H W, QUEK S T. Simulation of strongly non-Gaussian processes using Karhunen–Loeve expansion[J]. Probabilistic Engineering Mechanics, 2005, 20(2): 188−198.

[10] SCHUELLER G I, JENSEN H A. Computational methods in optimization considering uncertainties–an overview[J]. Computer Methods in Applied Mechanics and Engineering, 2008, 198(1): 2−13.

[11] LI Dian-qing, XIAO Te, CAO Zi-jun, et al. Slope risk assessment using efficient random finite element method[J]. Rock and Soil Mechanics, 2016, 37(7): 1994−2003.

[12] HUANG J, LYAMIN A V, GRIFFITHS D V, et al. Quantitative risk assessment of landslide by limit analysis and random fields[J]. Computers and Geotechnics, 2013, 53: 60−67.

[13] CHO S E. Probabilistic assessment of slope stability that considers the spatial variability of soil properties[J]. Journal of Geotechnical & Geoenvironmental Engineering, 2010, 136(7): 975−984.

[14] CHEN Zhao-hui, LEI Jian, HUANG Jing-hua, et al. Finite element limit analysis of slope stability considering spatial variability of soil strengths[J]. Chinese Journal of Geotechnical Engineering, 2018, 40(6): 985−993.

[15] TAN Xiao-hui, DONG Xiao-le, FEI Suo-zhu, et al. Reliability analysis method based on KL expansion and its application[J]. Chinese Journal of Geotechnical Engineering, 2020, 42(5): 808−816.

[16] CHO S E. Effects of spatial variability of soil properties on slope stability[J]. Engineering Geology, 2007, 92(3/4): 97−109.

[17] LIU Qian, ZHANG Xu-fang. A Chebyshev polynomial-based Galerkin method for the discretization of spatially varying random properties[J]. Acta Mechanica, 2017, 228(6): 2063−2081.

[18] JIANG Shui-hua, LIU Xian, YAO Chi, et al. System reliability analysis of rock slopes at low probability levels[J]. Rock and Soil Mechanics, 2018, 39(8): 2991−3000.

[19] PAPAIOANNOU IASON, BETZ WOLFGANG, ZWIRGLMAIER KILIAN, et al. MCMC algorithms for subset simulation[J]. Probabilistic Engineering Mechanics, 2015, 41: 89−103.

[20] HUANG J, FENTON G, GRIFFITHS D V, et al. On the efficient estimation of small failure probability in slopes[J]. Landslides, 2017, 14(2): 491−498.

[21] ZHANG Hao, YU Wei-wei, LIN Hang, et al. Analysis of location distribution of slope slip plane with different factors of safety[J]. Rock and Soil Mechanics, 2012, 33(2): 134−137, 160.